2011

Assessing the viability of sol-gel nimgo films for solar blind detection

Amber Scheurer
University of Central Florida

ASSESSING THE VIABILITY OF SOL-GEL NiMgO FILMS FOR SOLAR BLIND DETECTION

by

AMBER L. SCHEURER

A thesis submitted in partial fulfillment of the requirements
for the Honors in the Major Program in Electrical Engineering
in the College of Engineering and Computer Science
and in The Burnett Honors College
at the University of Central Florida
Orlando, Florida

Spring Term 2011

Thesis Chair: Dr. Winston V. Schoenfeld

ABSTRACT

Wide bandgap semiconductors have been broadly investigated for their potential to detect and emit high energy ultraviolet (UV) photons. Advancements in deep UV optoelectronic materials would enable the efficient and affordable realization of many medical, industrial and consumer UV optical devices. The traditional growth method, vacuum deposition, is an extremely complicated and expensive process. Sol-gel processing dramatically simplifies facility requirements and can be scaled to industrial size. The work presented here involves a novel study of the ternary wide bandgap material $Ni_{1-x}Mg_xO$. Films were developed by sol-gel spin coating for investigation of material and electrical properties.

This method produced films 200-600 nm thick with surface roughness below 4 nm RMS. Sintered films indicated an improvement from 60% to 90% transmission near the band edge. Additionally, compositional analysis was performed by X-ray Photoelectron Spectroscopy and film defects were characterized by photoluminescence using a continuous wave He-Cd UV laser, revealing the expected oxygen defect at 413nm. This film growth technique has produced thin polycrystalline films with low surface roughness and a high degree of crystalline orientation; crucial characteristics for semiconductor devices. These films have demonstrated the ability to be tuned over the full compositional range from the bandgap of NiO (3.6 eV) to that of MgO (7.8 eV). Optoelectronic devices produced by standard photolithographic techniques are discussed as well as the electrical transport properties of their metal contacts. Based on initial results, these films have demonstrated strong potential as solar blind detectors of UV radiation.

DEDICATION

To my parents, who have inspired, motivated, and taught me to truly believe I can do anything.

ACKNOWLEDGMENTS

I would like to express my deepest gratitude and most sincere thanks to all of the people who have made this project a possibility and who have helped me so much along the way.

My first research mentor, Dr. Jeremy W. Mares, taught me an incredible amount. I cannot thank him enough for his patience, encouragement, and camaraderie.

I have also had the privilege to work alongside and learn from Casey Boutwell. He has been the greatest source of knowledge and support through every stage of this project. I will always be grateful for his guidance, friendship, and inspiration.

To my thesis committee members, Dr. Kevin Coffey and Dr. Kalpathy Sundaram, I truly appreciate your time and your insight.

I would like to express great appreciation to my thesis chair and research advisor Dr. Winston V. Schoenfeld, whom I hold in the highest regard. He has provided me with innumerable opportunities as a member of his research group and has been extremely supportive in all of my endeavors.

Finally, thank you to my parents for your constant praise and your love, thank you to my friends for your companionship, and thank you to John for your unwavering support in all that I do.

TABLE OF CONTENTS

LIST OF FIGURES

INTRODUCTION

Wide bandgap semiconductors are of central interest for deep-ultraviolet (DUV) technologies. These materials absorb photons with energies larger than the bandgap, and are transparent to visible and infrared light because they do not provide enough energy to allow for transitions. Detectors that respond to wavelengths from about 280 nm and below are considered "solar blind" because that light from the sun is absorbed by our atmosphere [1]. Figure 1 shows the range of the solar spectrum due to atmospheric attenuation.

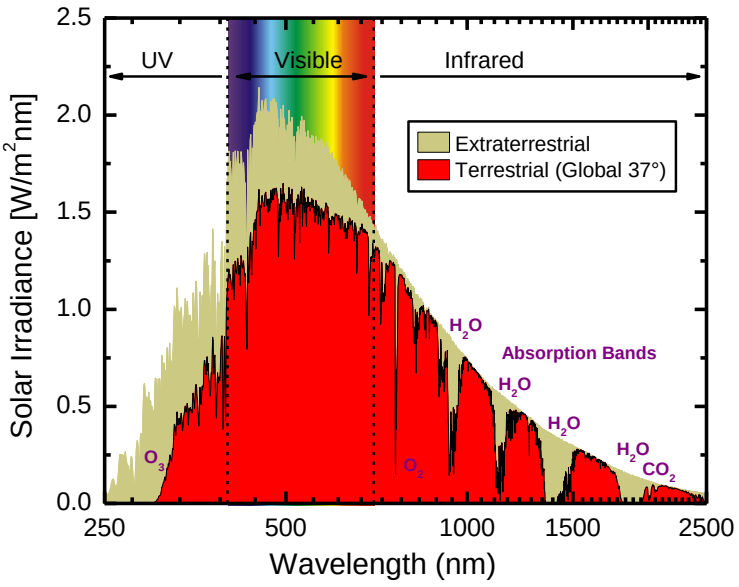

Figure 1: The terrestrial and extraterrestrial solar spectrum [2]

Among the many avenues into the DUV that are being researched, binary and ternary oxides have been among the notable candidates. Successes with ZnO (Eg = 3.37 eV) films in particular show tremendous promise for near UV applications and have already been exploited as

such [3]. However, to reach deeper into the UV, alternative materials with bandgaps in the 200 – 280 nm spectral region must be investigated.

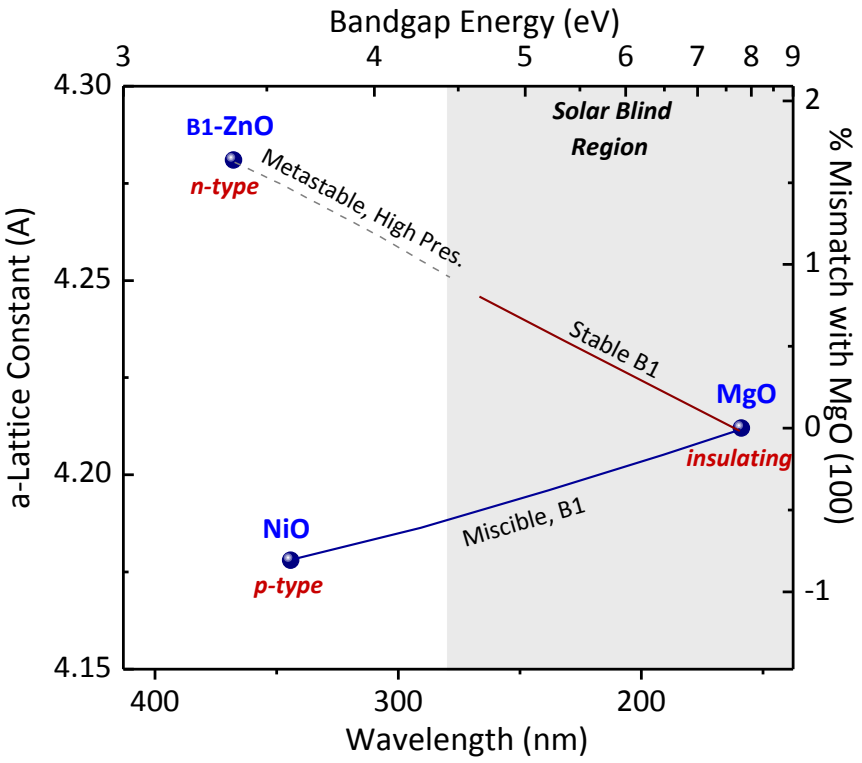

Figure 2: The bandgap tunability and lattice mismatch of selected oxide binary compounds [2]

The wide bandgap material under investigation in this study is $Ni_{1-x}Mg_xO$. Bandgap tunability in the deep-ultraviolet range has been demonstrated here as a function of the magnesium concentration, x [3]. The bandgap values that are accessible with this combination range from 3.6-7.8 eV, the bandgap of NiO to MgO respectively. Ultimately, the bandgap tunability in this region is due to the similarities in crystal structure as evidenced by lattice mismatch shown in Figure 2. This allows the NiO and MgO to easily form homogenous ternary compounds. Epitaxial growth of $Ni_{1-x}Mg_xO$ has been demonstrated using plasma-assisted molecular beam epitaxy (MBE), and these high quality films have shown responsivity in the

DUV range [4]. The sol-gel method is investigated here due to its economic and industrial feasibility.

MOTIVATION

Sufficient advancement in DUV optoelectronics will enable development of UV medical devices, high-density optical data storage, solar blind detection and important water purification technologies [5-7]. Specific military and industrial detection applications include combustion monitoring, air quality assessment, chemical sensors, and enhanced satellite communications [1]. In order to develop these applications, research in wide bandgap semiconductors must produce high quality films with reproducible electrical characteristics.

There are several proven growth methods available for semiconductor thin films including Molecular Beam Epitaxy (MBE), Metal-Organic Chemical Vapor Deposition (MOCVD), and Pulsed Laser Deposition (PLD) as well as sputtering and various dip-coating and sol-gel techniques [8-11]. Many of these processes are very expensive, particularly those requiring high vacuum like MBE and PLD. This investment can be justified by the potential to yield extremely high quality films, thus presenting the relationship between cost and performance.

Oppositely, a sol-gel spin-coating technique requires relatively inexpensive materials and minimal capital investment. Sol-gel provides the opportunity to further investigate the properties of $Ni_{1-x}Mg_xO$ and its ability to function as a useful material for solar blind detectors. Ultimately, sol-gel $Ni_{1-x}Mg_xO$ may prove to be a lower cost and more effective route to solar blind operation when compared to previously investigated semiconductors, but the viability and performance of sol-gel synthesized $Ni_{1-x}Mg_xO$ remains to be fully investigated [8].

EXPERIMENTAL METHODS

Material Growth Dynamics

In order to accurately design these optical thin films, thorough understanding of both the sol and film growth dynamics was required. The term sol refers to a liquid containing suspended particles, which is considered to be colloidal because the gravitational force on the particles is negligible [12]. Once the sol has been established, the next steps in the film growth process involve aging the sol, spinning, and sintering. Aging is the period of time in which gelation occurs, as shown in the box of Figure 3. During gelation larger molecules are created as bonds form between the particles, this is also called polymerization [12].

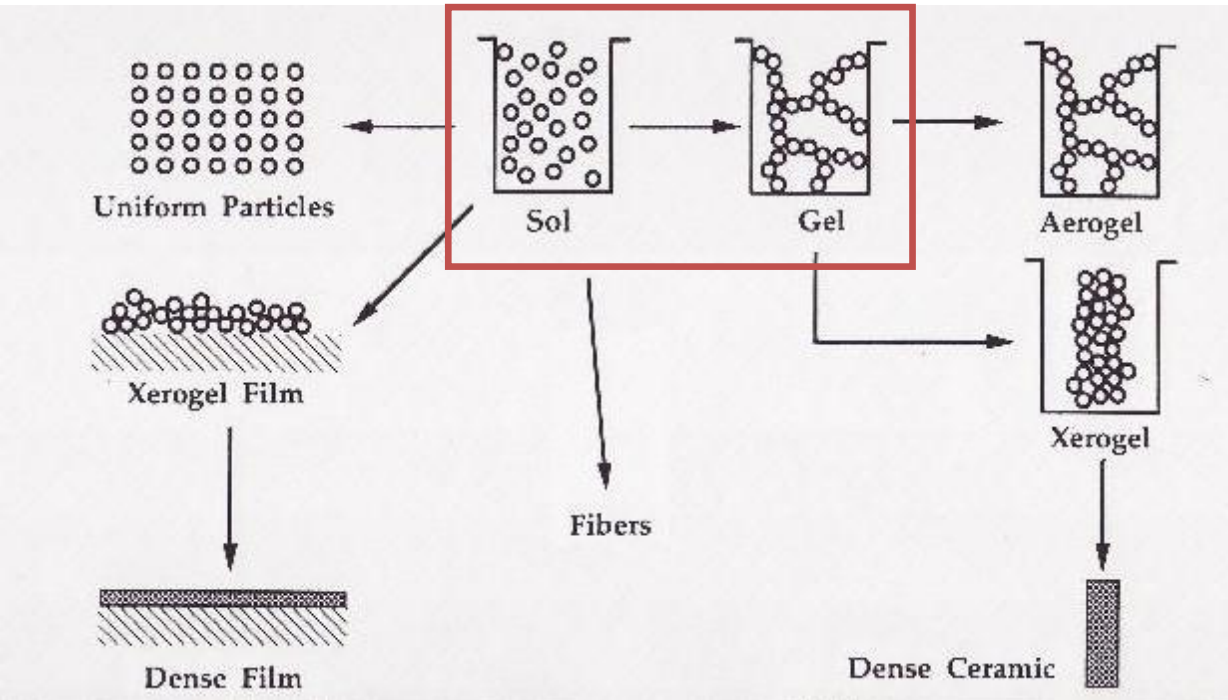

Figure 3: Overview of sol-gel processing [12]

Spin coating and dip coating are two of the most common methods for sol-gel film development. Dip coating involves the use of a stepper motor to slowly pull the substrate out of the mixture, coating it on both sides and making it ideal for arbitrary shaped substrates. This presents a challenge for post-processing and specifically makes it difficult to bake at high temperatures because of the material on both sides of the sample. Spin coating is advantageous in this regard because the sol is only applied to the top of the substrate and gives the user the ability to adjust the thickness of the film based on spin speed.

Sintering is a way of baking the film and helps improve optical properties by reducing defects and increasing crystalline size. This occurs because the films collapse and mix under the high temperatures, filling in vacancies and displacing interstitials that may have existed in the unsintered film.

Sol Mixture Development

In order to create sols of varying concentrations, different proportions of magnesium acetate and nickel acetate precursors were combined for a total mass of 1 gram. These precursors were dissolved in 20 ml of 2-methoxyethanol by placing the beaker on a hotplate at 60°C with a stir-bar at 400 RPM for 1 hour. In some iterations of the growth process, the sol stabilizer diethanolamine (DEA) was added to the mixture to help promote uniformity throughout the sol.

Aging

Upon removal from the hotplate, the beaker containing the sol was covered and allowed to age for 24 hours. Aging times ranging from 0-100 hours were investigated to determine optimal sol formation. Aging for 24 hours was chosen in this experiment because longer times

did not show significant improvement in crystallite size and shorter times did not allow for thorough gelation.

Spinning

Before spinning, 1” quartz substrates were cleaned in an ultrasonic bath of acetone, followed by isopropyl alcohol, then deionized water and dried under nitrogen flow. The substrate was then placed on a Laurell WS-650Sz Series Lite Spin Processor, where the sol was applied with a disposable plastic pipette. Samples were spun at 2000 RPM for 30 seconds or 5000 RPM for 60 seconds depending on intended thickness and cooling expectations. In between layers, samples were baked on a hotplate at temperatures ranging from 100°C to 300°C for 2 to 10 minutes and allowed to cool for 3 to 10 minutes. This was then repeated 7 to 10 times, depending on sol age and spin speed. These parameters were determined after several trials to eliminate cracking in the film which can occur during drying.

Sintering

Following the growth procedures, films were heated to 600°C, 800°C, or 1000°C in an MTI Corporation GSL1100X furnace for 2 hours. In order to control the flow of air, a mechanical pump was used to reduce the furnace chamber pressure, regulating cooling air flow with an MTI flow meter. During the sintering process, the air pressure was maintained at 1 atm with a flow rate of 1 L/min.

Growth Characterization

Several methods were utilized to verify the progress and results of the film growth techniques described above. Each process provided significant real time insight into the material properties and allowed for dynamic evolution of the growth technique between experimental iterations.

Film Thickness

In order to assess film thickness, layers were measured using a Veeco Dektak 150 profilometer. A small scratch was first made in the film, exposing the substrate below. The profilometer then measured the scratch depth in relation to the film surface, providing the thickness. This scratch test was useful in understanding the effects of various spin speeds and determining how many layers to apply. Additional information about surface roughness and particle inclusion can also be determined by profilometry, providing insight into macroscopic defect growth.

Surface Morphology

Using a Digital Instruments Dimension 3100 Atomic Force Microscope (AFM) the surface structure of the films can be characterized. This machine uses a laser reflected from a vibrating silicon cantilever in tapping mode which reveals the surface structure and RMS roughness. This is a good indicator of film quality and can be an initial checkpoint before continuing with fabrication.

Optical Transmission

A Cary 500 UV-Vis-NIR Spectrophotometer was used to determine the optical properties of the films. The spectrophotometer measured the light that was transmitted through the film as a function of incident photon energy. This investigation revealed the energy at which the film began absorbing radiation, indicating the onset of the absorption edge and reduced transmission. This absorption edge is typically at the bandgap of the semiconductor thin film.

Compositional Analysis

X-Ray Photoelectron Spectroscopy (XPS) was used to verify the composition. This technique involves irradiation of the sample with x-rays and interpretation of the range of energies of the emitted photoelectrons. Each element has specific electron binding energies which create a type of signature. The composition of the film was determined by correlating the measured with expected photoelectron energies.

Crystallographic Analysis

Further material analysis was performed using a Rigaku D/MAX II X-Ray Diffraction (XRD) system to investigate lattice spacing and crystalline orientation. This technique involves a collimated beam of x-rays reaching the surface of the film, penetrating the first few monolayers and diffracting out. This angle of diffraction is then used to determine the material properties by measuring diffracted peak position and peak width. The resulting data can be interpreted to better understand the lattice spacing, crystal structure, and crystal quality of the sample under investigation; parameters which are crucial for thin film growth and semiconductor properties.

Defect Characterization

Additionally, photoluminescence studies were performed using a continuous wave He-Cd laser (325 nm). This laser was used for defect analysis because it lases at a lower energy than the bandgap of the film so there is no band emission from the semiconductor material. This is useful because the laser will excite many of the defects which exist in the bandgap, providing further insight into the material quality and properties.

RESULTS AND DISCUSSION

The majority of the films produced were between 200 and 600 nm as measured by profilometry, constituting 7 to 10 layers. This thickness was sufficient for processing and testing the films without being so large that they crack from stress while drying. Sintering provided a significant improvement in film quality and is evident in the steep band edge shown in Figure 4. The films show improvement in transmission from 65% in the unsintered case to over 90% in those sintered at 800°C. Furthermore, the films sintered at 600°C and 800°C demonstrated lower RMS Roughness values (< 1 nm) as compared to either the 1000°C trial or the unsintered sample. As predicted, sintering allowed for the films to collapse and mix, thus improving their crystalline qualities.

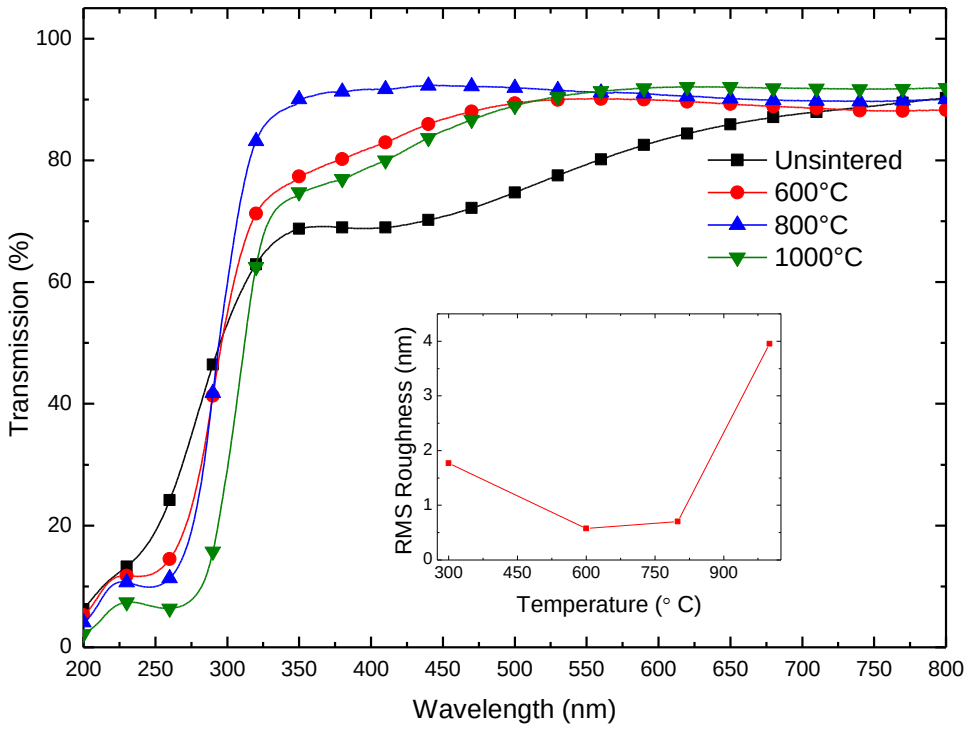

Figure 4: Variation in percent optical transmission as a function of sintering temperature for $Ni_{0.5}Mg_{0.5}O$

The correlation between the decreased transmission of the 1000°C sintered film and its increased surface roughness indicates that surface deformation occurs between 800°C and 1000°C. Using these films as detectors requires metal contact fabrication and makes low RMS roughness ideal. The $Ni_{0.5}Mg_{0.5}O$ film shown in Figure 5 was produced after sintering at 800°C with RMS roughness = 0.701 nm.

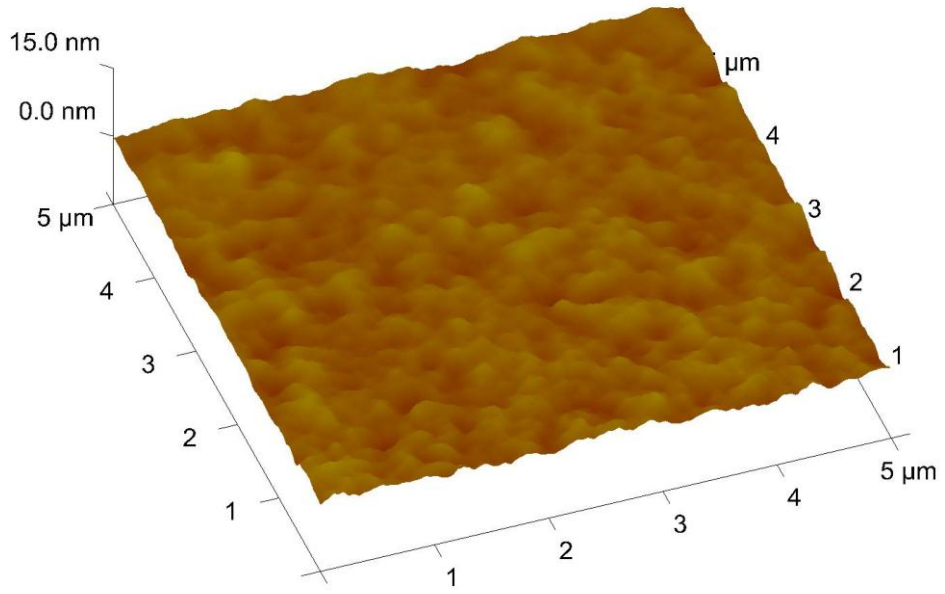

Figure 5: AFM image of $Ni_{0.5}Mg_{0.5}O$ film after sintering at 800°C for 2 hours, RMS roughness = 0.701 nm

Figure 6 establishes the bandgap tunability of $Ni_{1-x}Mg_xO$ as a function of magnesium concentration, x. The results presented in this figure are of films sintered at 800°C in air for 2 hours with increasing concentrations of magnesium, beginning with x=0 (pure NiO) and ending with x=1 (pure MgO). As predicted, the increase in magnesium concentration caused a blue-shift in the transmission and validates the theory of sol-gel $Ni_{1-x}Mg_xO$ bandgap tunability.

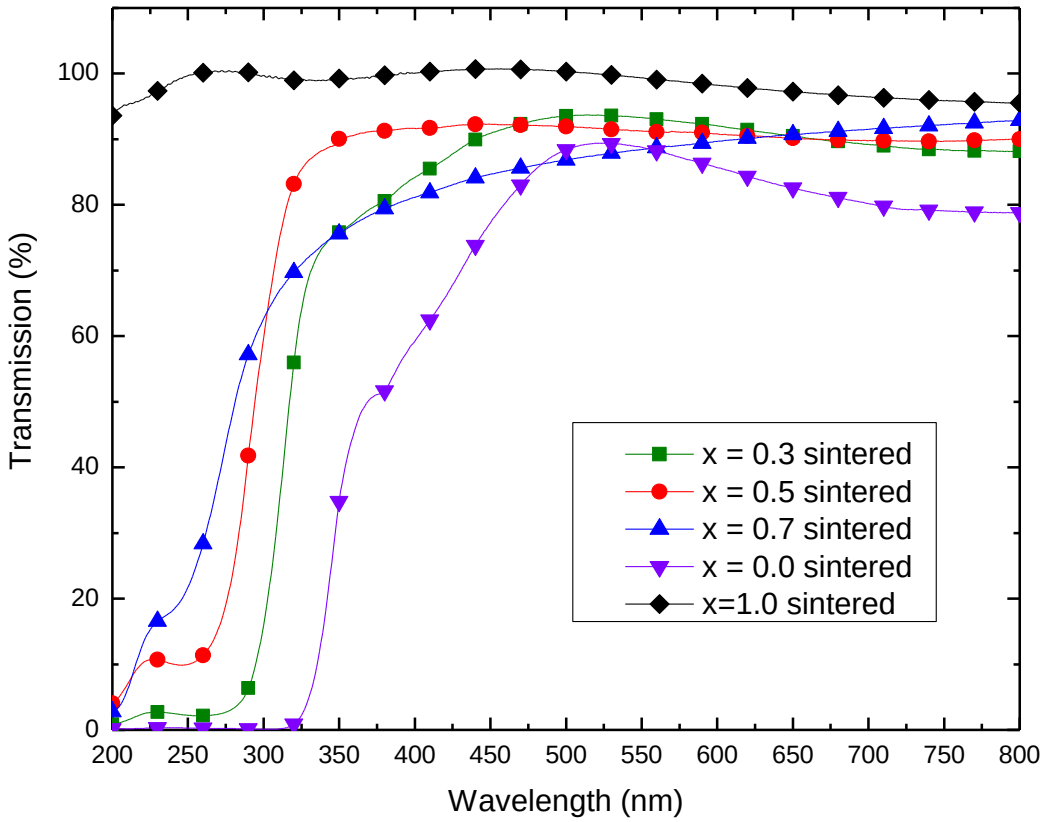

Figure 6: Bandgap tunability of $Ni_{1-x}Mg_xO$ as a function of magnesium concentration, x

The results presented here are further vindicated when compared to the other published literature on $Ni_{1-x}Mg_xO$ as shown in Figure 7. A majority of reported investigations indicate a nonlinearity in bandgap tunability, as supported by this study.

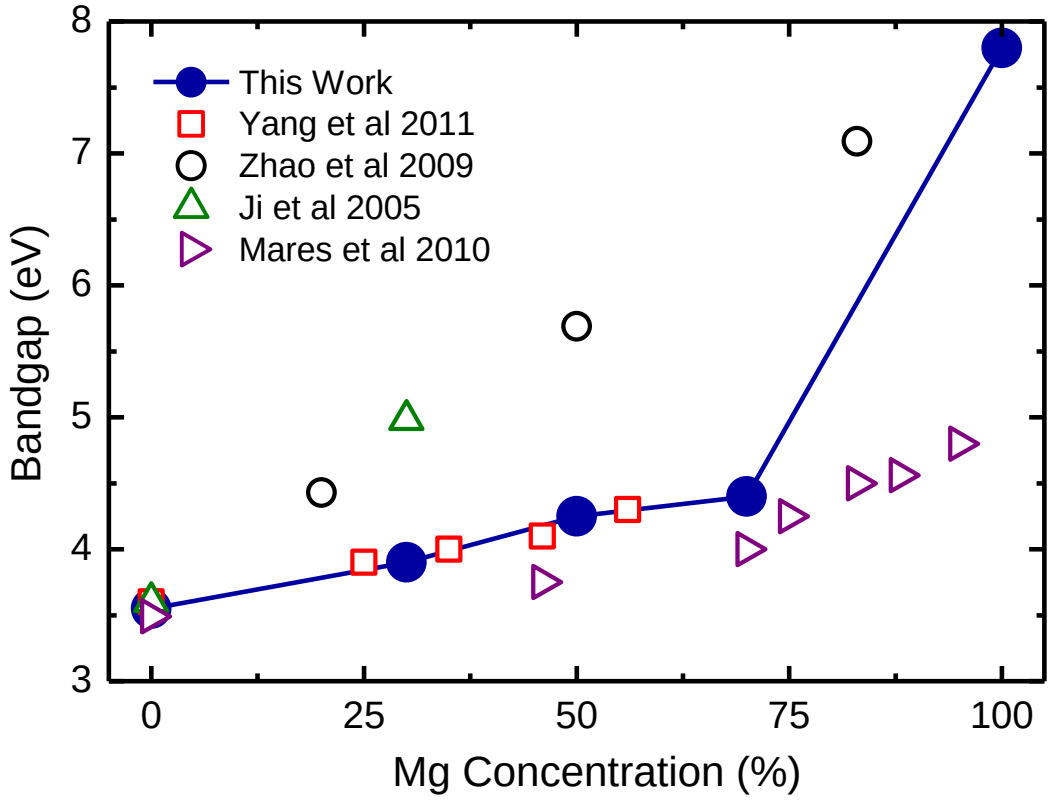

Figure 7: Bandgap of NiMgO in comparison to recent studies [8, 13-15]

The composition of the film, as investigated using XPS analysis, indicated that the proportions of the precursors present in the initial sols were very similar to the ratio of metal incorporation in the films. Ultimately, this encouraging result confirms that using the sol-gel process, a near-linear relationship between the input precursor ratio and the compositional output of the film can be obtained.

The full shift in the lattice constant evident in the XRD data presented in Figure 8 is also a reproduction of results that have previously been obtained from single crystal films. The full width at half maximum (FWHM) of the diffracted peaks became narrower with decreasing Mg incorporation indicating larger grain size in the polycrystalline film. The linearity of the increase

in lattice spacing in relation to the increase in magnesium concentration is another promising observation, supporting Vegard's Law and simplifying lattice engineering.

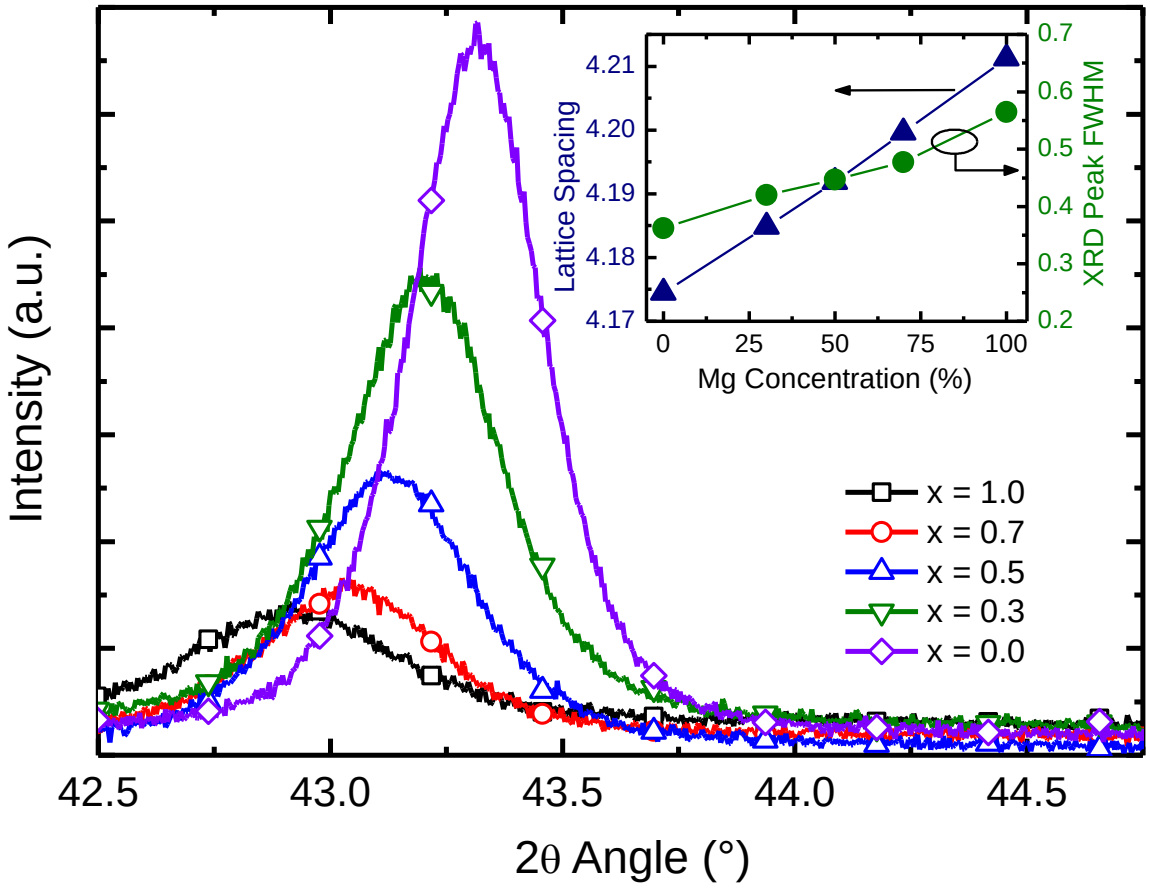

Figure 8: XRD and Lattice Parameter for $Ni_{1-x}Mg_xO$ [16]

When performing photoluminescence (PL), it was expected that there would be an oxygen defect near 413 nm [17]. Test results supported this as an emission was observed in this region and was more intense following sintering which further supports the oxygen defect explanation. Further investigation of this defect will improve film quality and improve detector responsivity.

Overall, the results of the material investigation are very encouraging. The spin coating sol-gel method has produced consistent tunable $Ni_{1-x}Mg_xO$ films. Characterization of these films includes investigation in surface morphology, lattice spacing, and optical transmission, all of which support the band edge tunability of $Ni_{1-x}Mg_xO$. Sol-gel $Ni_{1-x}Mg_xO$ provides an inexpensive alternative to traditional semiconductor materials and growth methods and shows great promise for use in solar blind optoelectronic devices.

ONGOING RESEARCH

The electrical characteristics must be examined in order to further investigate sol-gel $Ni_{1-x}Mg_xO$ for use as UV detectors. Previous investigations into contact fabrication and device characterization have been performed on single crystal $Ni_{1-x}Mg_xO$ and will be reproduced with modification for this study. Additional research into semiconductor doping is anticipated as well. Lithium has been identified as a potential dopant although it is small and highly mobile, making it difficult to place into the crystal, especially when sintering is an important part of the film growth process.

Contact Fabrication

In order to perform device testing, the fabrication process needs to be characterized because the ability to consistently fabricate contacts is imperative. As with the actual film growth dynamics, the contact fabrication involves many stages of experimentation in the methodology before the devices created can be used.

For this study, the fabrication facility consists of a class 100 clean room located within a class 1000 clean room. It is anticipated that standard photolithographic techniques will be used, as have been demonstrated in previous studies. Individual spinning, baking, and exposure times will be adjusted as necessary.

The contact metal used to create the devices will also be under scrutiny. Both low resistance Ohmic and rectifying Schottky contacts will be considered and evaluated for advantages in the contact metal characterization. Metals will be deposited via electron beam

evaporation or thermal evaporation and heated in a rapid thermal annealer to promote mixing of the contact metals.

Device Design

An interdigitated metal-semiconductor-metal (MSM) device design with finger spacing ranging from 1-15 µm has been created using L-Edit software and fabricated in-house using the Leica electron beam lithography tool. Figure 9 depicts the mask design and shows both the MSM designs as well as the contact style known as transfer length measurement (TLM) patterns. Two versions of this mask have been created for use with either positive or negative photoresist.

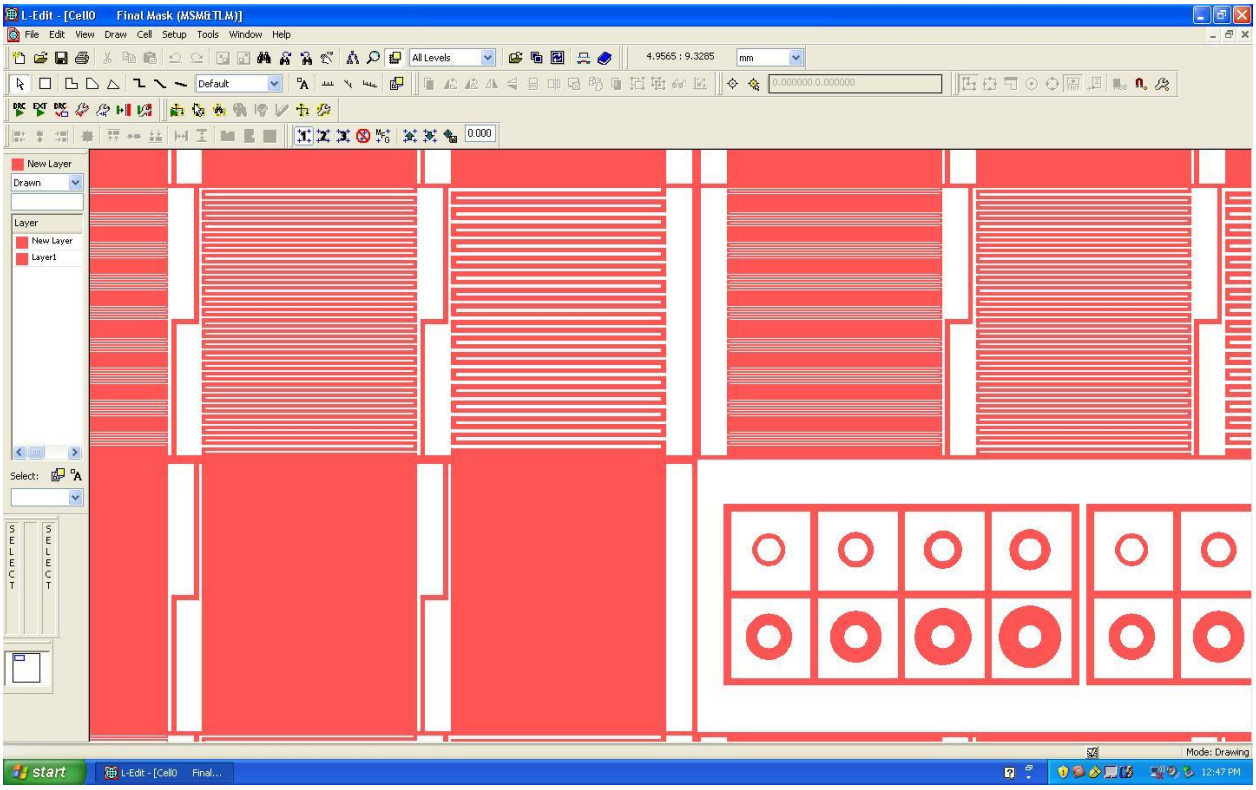

Figure 9: Screenshot of photomask design in L-Edit software

The MSM layout was chosen as the device architecture for this experiment because it functions as a simple photodetector. The resistance of the device is reduced when it is exposed to

the light of energy larger than the bandgap. The fingers extend from a pad on each side providing a contact for the probes used in testing. Figure 10 shows the MSM device in more detail, including the inset which shows a fabricated device with 1 µm spacing. The referenced finger spacing refers not only to the spacing between fingers but also to the size of the fingers themselves.

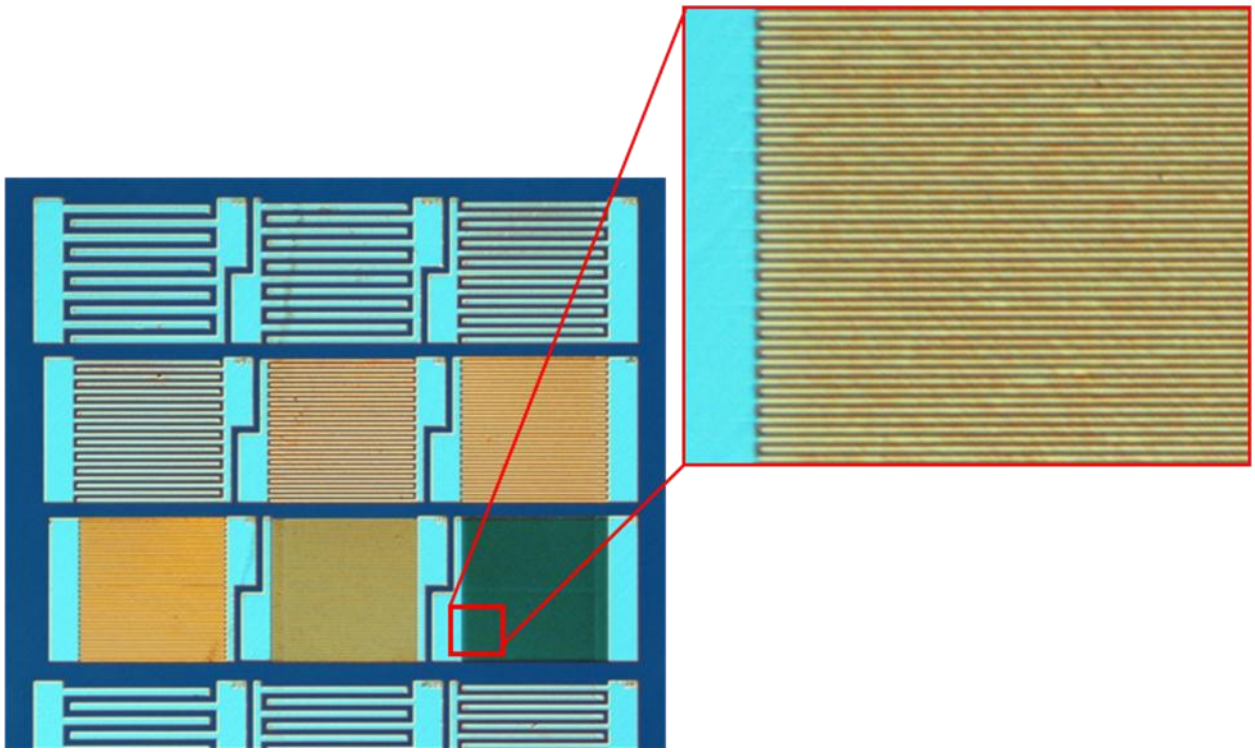

Figure 10: MSM devices with finger spacing from 1-15 µm, insert shows 1 µm spacing

Device Characterization

Several methods are used to test the electrical properties of the device through various stages of contact fabrication and afterwards. When used in conjunction with a probe station, the Keithly 2400 SourceMeter allows for current-voltage (IV) testing of the device. This will give insight into the resistance of the film in varying fabrication conditions. The sourcemeter's probes

are placed on the metal pads that connect to the interdigitated fingers as depicted in Figure 11, allowing for IV measurement across the device.

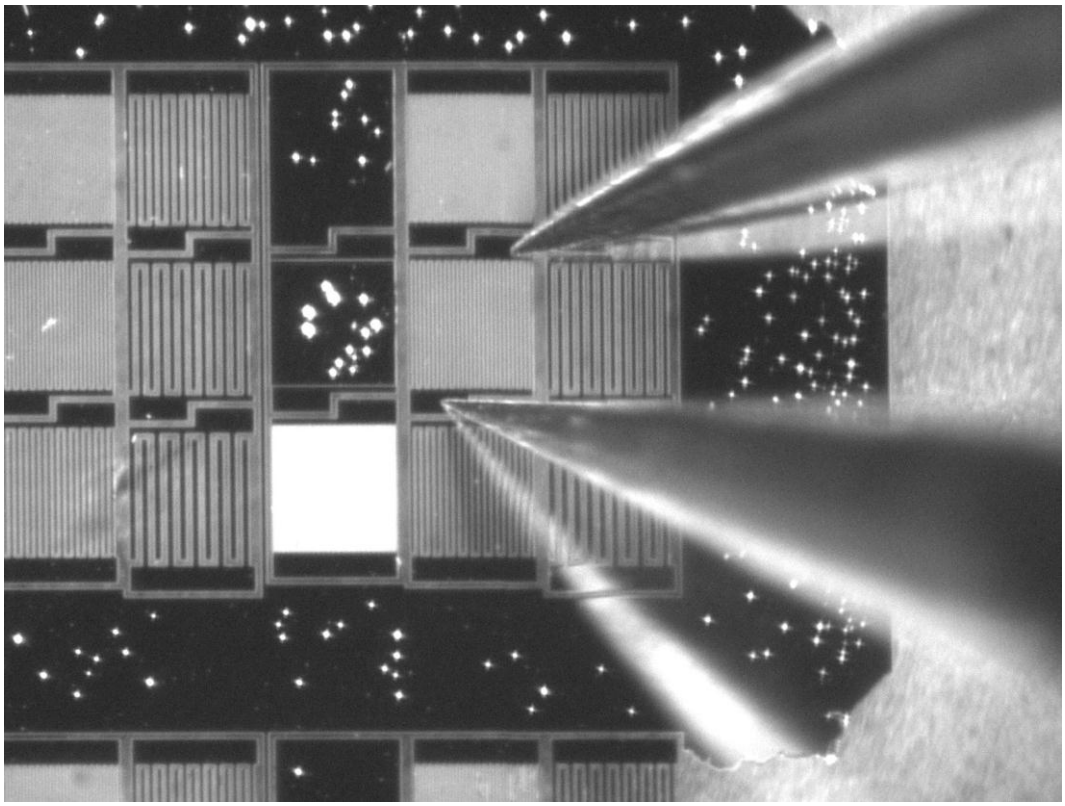

Figure 11: MSM device under IV testing using probe station

Additionally, spectral responsivity can be obtained using a spectrometer, monochrometer, xenon lamp, power meters, and sourcemeter. This set-up measures the output power from the device as a function of the light in. This has also been modified to measure the spectrotemporal response, investigating device responsivity with respect to exposed time.

Semiconductor doping will also require another important testing method, the Hall effect. This investigation can be performed over a range of temperatures. This will yield important doping information regarding the carrier type, carrier concentration, and resistance.

REFERENCES

1. Razeghi, M., *Short-wavelength solar-blind detectors - Status, prospects, and markets.* Proceedings of the IEEE, 2002. **90**(6): p. 1006-1014.
2. Mares, J.W., et al., *Molecular Beam Epitaxial Growth of Cubic Ternary Oxide Semiconductors for Deep UV Applications*, in *Photonics West*. 2010: San Francisco.
3. Chen, N.B. and C.H. Sui, *Recent progress in research on MgxZn1-xO alloys.* Materials Science and Engineering B-Solid State Materials for Advanced Technology, 2006. **126**(1): p. 16-21.
4. Mares, J.W., et al., *Deep-ultraviolet photodetectors from epitaxially grown $Ni_xMg_{1-x}O$.* Applied Physics Letters, 2010. **97**(16): p. 161113.
5. Bersillon, J.L., *Water purification and disinfection processes.* Acta Hydrochimica Et Hydrobiologica, 1999. **27**(2): p. 98-100.
6. Oppenlander, T., et al., *Novel vacuum-UV-(VUV) and UV-excimer flow-through photoreactors for waste water treatment and for wavelength-selective photochemistry.* Proceedings of the Indian Academy of Sciences-Chemical Sciences, 1995. **107**(6): p. 621-636.
7. Talu, G.F. and V. Diyamandoglu, *Formate ion decomposition in water under UV irradiation at 253.7 nm.* Environmental Science & Technology, 2004. **38**(14): p. 3984-3993.
8. Ji, Z., et al., *Synthesis of $Mg_xNi_{1-x}O$ thin fimls with a band-gap in the solar-blind region.* Journal of Crystal Growth, 2005. **273**: p. 446-450.

9. Kaufmann, T., et al., *Mocvd Layer Growth of Zno Using Adducts of Dimethylzinc and Diethylzinc.* Crystal Research and Technology, 1989. **24**(3): p. 269-274.

10. Yadavalli, S., M.H. Yang, and C.P. Flynn, *Low-Temperature Growth of Mgo by Molecular-Beam Epitaxy.* Physical Review B, 1990. **41**(11): p. 7961-7963.

11. Fork, D.K., et al., *Epitaxial Mgo on Si(001) for Y-Ba-Cu-O Thin-Film Growth by Pulsed Laser Deposition.* Applied Physics Letters, 1991. **58**(20): p. 2294-2296.

12. Brinker, C.J. and G.W. Scherer, *Sol-Gel Science: The Physics and Chemistry of Sol-Gel Processing*. 1990, San Diego: Academic Press, Inc.

13. Mares, J.W., et al., *Cubic ZnxMg1-xO thin films grown by plasma-assisted molecular-beam epitaxy for optoelectronic applications.* Journal of Materials Research, 2010. **25**(6): p. 1072-1079.

14. Yang, Z.-G., et al., *Preparation and band-gap modulation in $Mg_xNi_{1-x}O$ thin films as a function of Mg contents.* Thin Solid Films, 2010.

15. Zhao, Y.M., et al., *MgNiO-based metal-semiconductor-metal ultraviolet photodetector.* Journal of Physics D-Applied Physics, 2009. **42**(9).

16. Boutwell, R.C., et al., *NiMgO Thin Films by Sol-Gel Spin Coating*. 2011, College of Optics and Photonics, CREOL: Orlando, FL.

17. Mochizuki, S. and T. Saito, *Intrinsic and defect-related luminescence of NiO.* Physica B-Condensed Matter, 2009. **404**(23-24): p. 4850-4853.